

## Internal Crack Initiation in High-cycle Fatigue of a Ti-Fe-O Alloy at Liquid Nitrogen Temperature

H. YOKOYAMA\*, O. UMEZAWA\*\*, K. NAGAI\*\*, T. SUZUKI\*, and K. KOKUBO\*

\* *Department of Mechanical Engineering, Kogakuin University*

*Nishi-shinjuku, Shinjuku, Tokyo 163-8677, Japan*

\*\**National Research Institute for Metals*

*Sengen, Tsukuba, Ibaraki 305-0047, Japan*

### ABSTRACT

By using scanning electron microscope equipped with EDS and 3D analyses, microstructure and crack initiation site of a Ti-Fe-O alloy were characterized in order to clarify the internal fatigue crack generation. Most of fatigue samples failed at 77 K exhibited internal crack initiation, but pre-existing defects were not detected in the vicinity of initiation sites. The alloy consisted of recovered  $\alpha$  grain and recrystallized  $\alpha$  grain. The internal crack initiation site consisted of single or plural facets. Facet was transgranularly formed, and was fitted to a recrystallized  $\alpha$  grain judging from its morphology, size, and chemistry.

*Key words:* high-cycle fatigue, fatigue crack initiation, transgranular cracking, near  $\alpha$ -type titanium alloy

### 1. INTRODUCTION

In general, fatigue crack initiation is understood to occur on the specimen surface owing to the irreversible process of extrusion and intrusion through slip deformation.<sup>1</sup> In titanium alloys, however, internal (subsurface) crack initiation not associated with pre-existing defects has been reported at and below room temperature, where the sites were highly crystallographic and the fracture mechanism was not explained by the simple extrusion-intrusion mechanism.<sup>2</sup> Crack initiation sites were distributed from specimen surface to center in Ti-Fe-O (near  $\alpha$ -type titanium) alloy, although there was a tendency for a favorable depth of the location in Ti-6Al-4V ( $\alpha$ - $\beta$  type titanium) alloys.<sup>3</sup> Deformation structure of  $\alpha$  phase in Ti-6Al-4V alloys were characterized and the crack initiation mechanism has been discussed.<sup>4,5</sup> Few characterization, however, have been made for the internal crack initiation sites of Ti-Fe-O alloy. Purpose of the present study is to characterize the crack initiation site in detail and to discuss microcracking and its growth from the viewpoints of fractography.

## 2. EXPERIMENTAL

## 2.1. MATERIALS

Test material is a rolled plate of a near  $\alpha$ -type Ti-Fe-O alloy. Its chemical compositions are given in Table 1.

Table 1 Chemical compositions of the test material.

Element	Fe	O	C	N	Ti
Concentration (wt%)	0.71	0.269	0.015	0.0158	Balance

The tensile properties at 77 K are given as follows; ultimate tensile strength:  $\sigma_B = 1292$  MPa, 0.2% proof stress:  $\sigma_y = 1165$  MPa, and total elongation: El= 20%.

Hourglass-shaped fatigue test specimens were machined parallel to the RD. Fatigue tests were carried out in liquid nitrogen (77 K).<sup>3</sup> Load-controlling test was performed with stress ratio,  $R = 0.01$ , in a sine wave. Figure 2 shows S-N data.<sup>3</sup> The specimens which showed internal crack initiation were intensively examined in the present study.

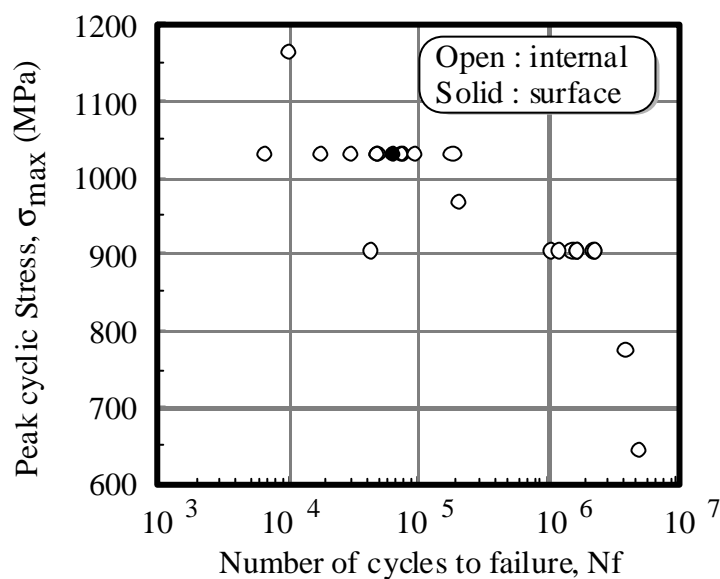


Fig. 1 S-N data of Ti-Fe-O alloy at 77 K.

## 2.2 ANALYSES

Fatigue crack initiation sites and fracture surfaces were characterized by scanning electron microscopy (SEM). Distribution of iron in both crack initiation site and microstructure was qualitatively analyzed by energy dispersive X-ray spectroscopy (EDS). Three-dimensional (3D) morphology of the initiation sites was analyzed by using a back-scattered electron device. Microstructure in the longitudinal section beneath fracture surface was also

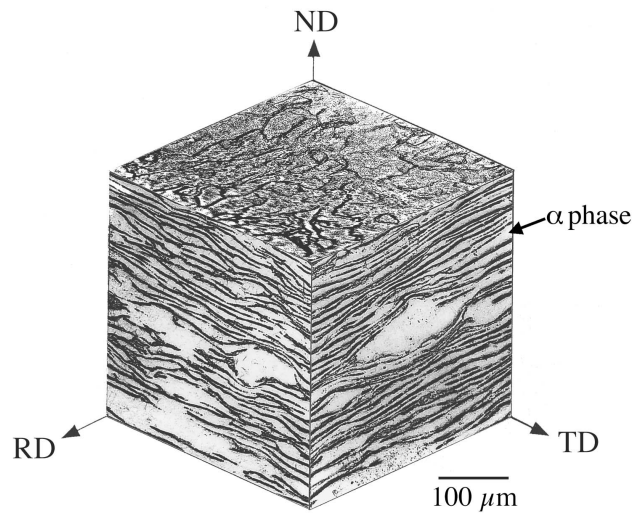


Fig. 2 Optical micrograph of Ti-Fe-O alloy.

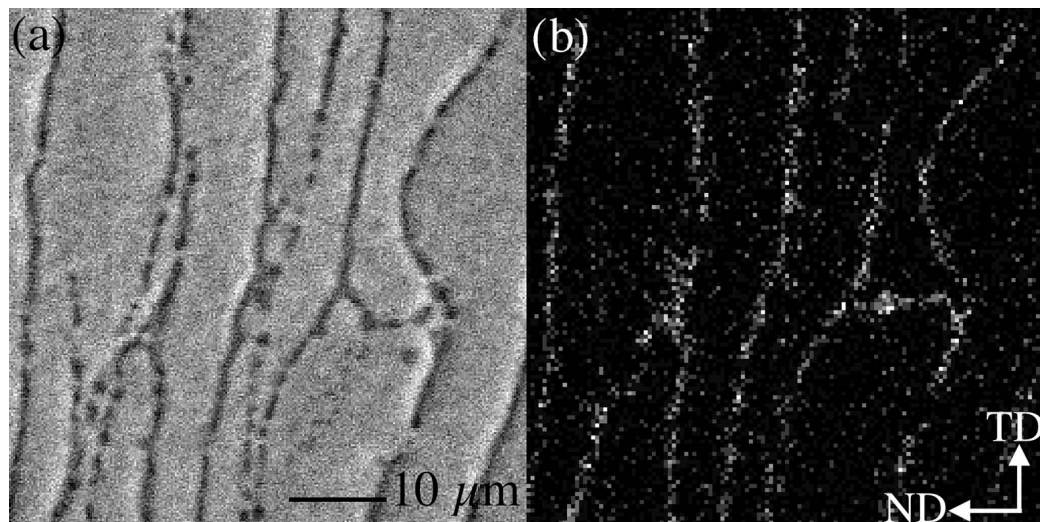


Fig. 3 Secondary electron image (a) and its iron mapping image by EDS (b) on the RD plane.

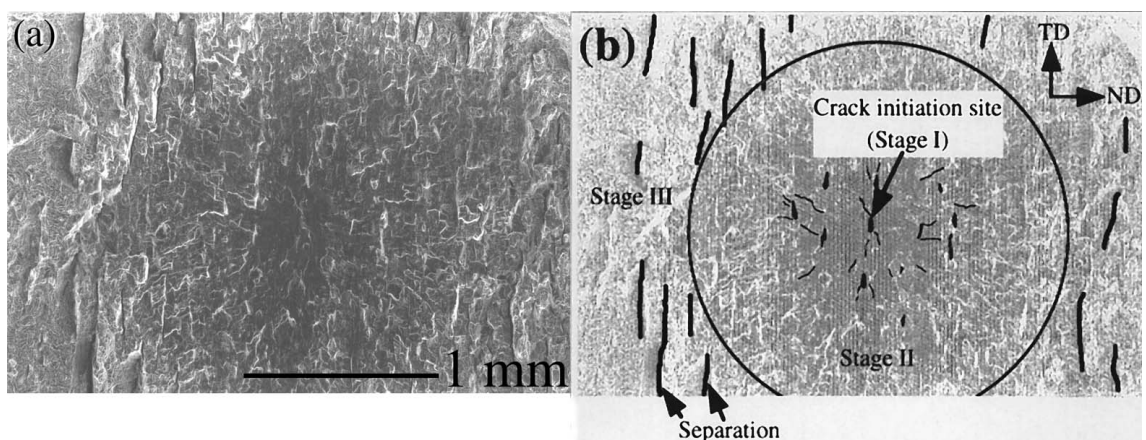


Fig. 4 SEM photographs of fracture surface for a sample showed internal crack initiation ( $\sigma_{\max} = 1033$  MPa,  $N_f = 74,650$  cycles): (a) fracture surface and (b) illustration of (a).

observed in order to detect sub-cracks.

### 3. RESULTS AND DISCUSSION

#### 3.1. MICROSTRUCTURE

Optical micrograph of the Ti-Fe-O alloy is represented in Fig. 2. The alloy consists of  $\alpha$  phase (white color area in Fig. 2) and fine  $\beta$  phase. Each  $\alpha$  grain is elongated parallel to both RD (rolling direction) and TD (transverse direction). The  $\alpha$  microstructure is classified into two regions, which are designated "recrystallized  $\alpha$  grain" and "recovered  $\alpha$  grain".<sup>6</sup> Grain width of recovered  $\alpha$  is about several micrometer, although that of recrystallized  $\alpha$  is about 20  $\mu\text{m}$ . Figure 3 shows iron analysis map for the test alloy on the RD plane. Concentrated iron exists at  $\alpha$  grain boundary discontinuously, which is fitted to  $\beta$  phase.

#### 3.2. FRACTURE SURFACE

No defects such as inclusion and pore are detected on fracture surface. As shown in Fig. 4, fracture surface is classified into three regions, i.e. Stage I, Stage II and Stage III. Fatigue crack initiates internally as a Stage I crack and is propagating in a radial pattern on Stage II. Crystallographic facets are also seen on Stage II. Crack initiation site, facets and separations are aligned along the TD.

#### 3.3. CRACK INITIATION SITE

Internal crack initiation sites consisted of single or plural facets. Figure 5 represents the matching-halves of an internal crack initiation site. The internal crack initiation site is a crystallographic facet with about 20  $\mu\text{m}$  width. Region A marked in Fig. 5(c) and (d) has no traces and/or protrusions, and contacts the edge of the initiation site. On the other hand, the rest of region A in the site, region B, shows traces or steps on the facet. The traces grow from region A in a radial pattern. Segregation of iron in the vicinity of crack initiation site is detected (Fig. 5(e)). As illustrated in Fig. 5(f), iron enriched region, i.e. lines  $yy'$  and  $zz'$ , are fitted to the edge of the facet. Region A touches the line  $yy'$  which is a recrystallized  $\alpha$  grain boundary. Judging from shape, size and iron distribution, facet (crack initiation site) is fitted to a recrystallized  $\alpha$  grain.

#### 3.4. 3D ANALYSIS

Figure 6 shows relative-height line profile of sections in the initiation site (facet) shown in Fig. 5(a) and (c). At low magnification (section between points 1 and 2), the facet is flat and is inclined to the principal stress axis with about 54 degrees. At high magnification (section between points 3 and 5), however, region A is not on the same plane with region B; the angle of refraction is about 2 degrees in Fig. 6(b).

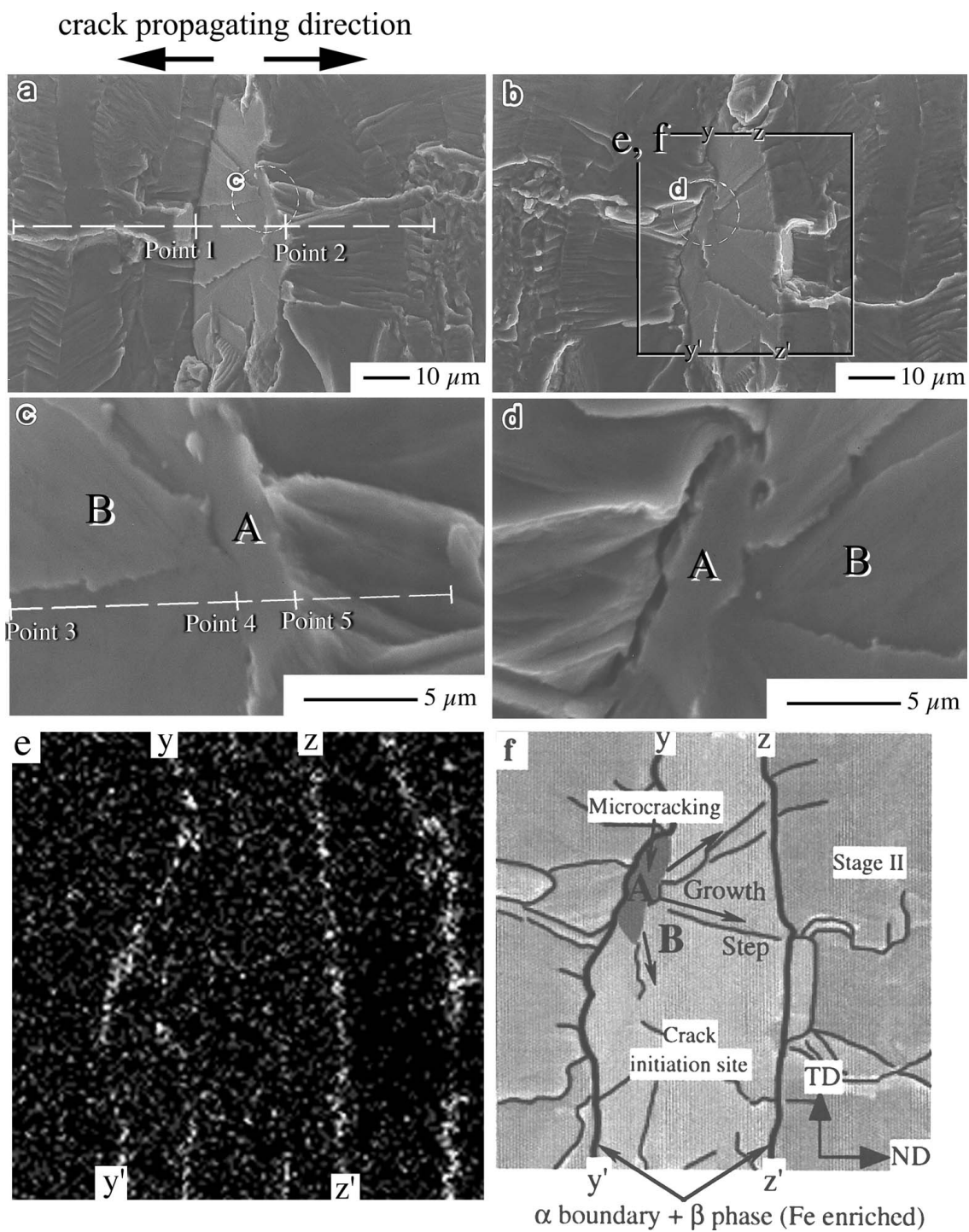


Fig. 5 Matching halves in the vicinity of an internal crack initiation site ( $\sigma_{\max} = 1033$  MPa,  $N_f = 186,590$  cycles). Photographs (c) and (d) are magnified images of photographs (a) and (b). Micrograph (e) is iron mapping image of (b) by EDS. Figure (f) is illustration of (b).

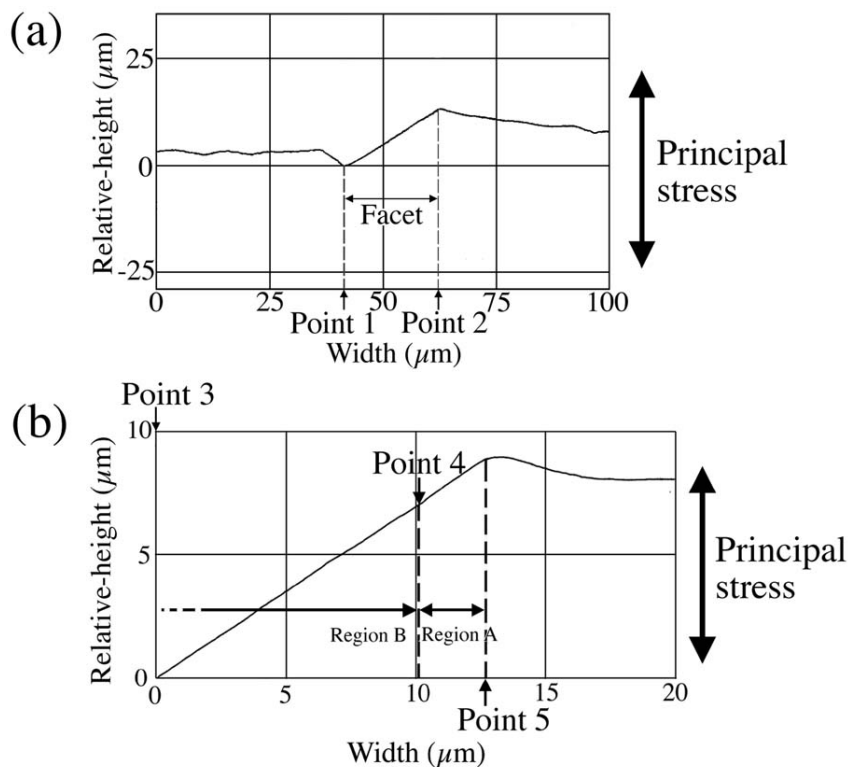


Fig. 6 The relative-height line profile of the internal crack initiation shown in Fig. 5(1) and (c).

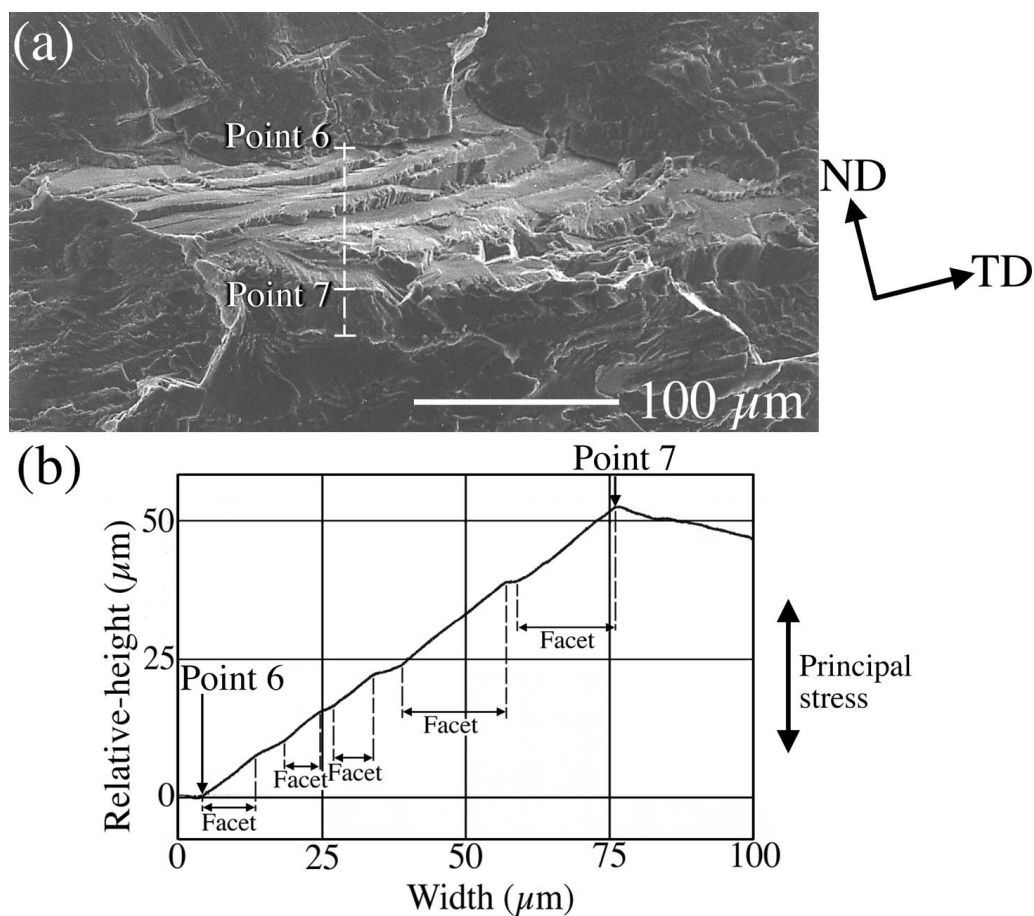


Fig. 7 SEM photograph of an internal crack initiation site at the lowest stress level (a) and the relative-height line profile of the site (b):  $\sigma_{\text{max}} = 646 \text{ MPa}$ ,  $N_f = 5,107,910$  cycles.

Figure 7 shows the internal crack initiation site of a sample of which was failed at the lowest applied stress level in the present study. Plural facets form this crack initiation site whose size is much greater than that at higher stress level. The slope of those facets in a section shown in Fig. 7(a) is almost the same between points 6 and 7 (Fig. 7(b)) at low magnification.

### 3.5. SUB-CRACK

Figure 8 shows sub-cracks on the TD plane (in the longitudinal section) for a fatigue fractured sample. A sub-crack with a length of about  $20\ \mu\text{m}$  is detected in a recrystallized  $\alpha$  grain, and is inclined to the principal stress axis with about 30 degrees. All of sub-cracks observed beneath fracture surface were transgranularly formed in the recrystallized  $\alpha$  grain.

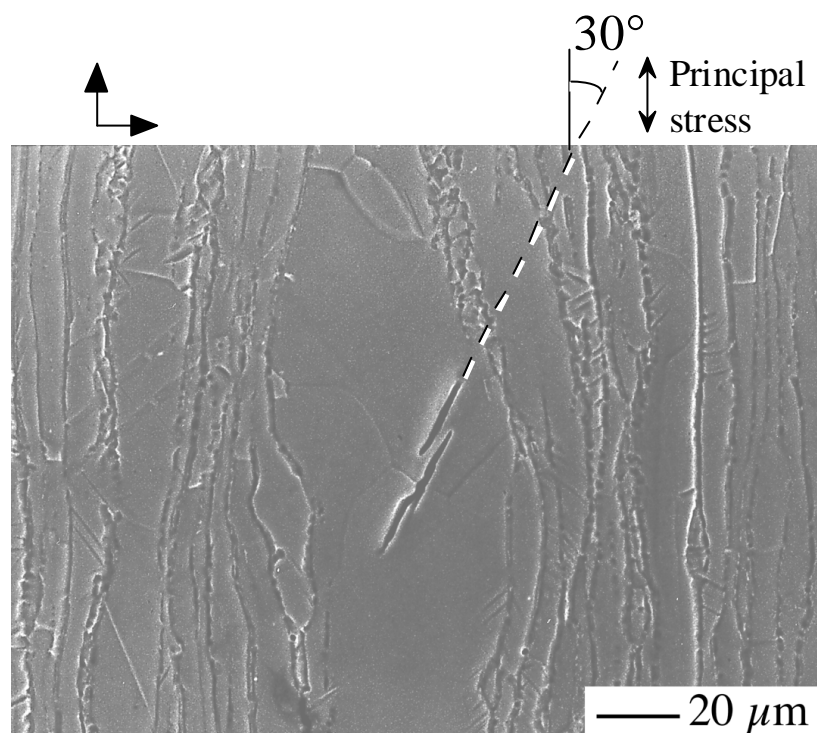


Fig. 8 Transgranular sub-crack formed in recrystallized  $\alpha$  grain on the TD plane.

### 3.6. INTERNAL CRACK GENERATION

Umezawa *et al.*<sup>5</sup> suggests that the internal crack initiation site in Ti-6Al-4V alloy was created by a process of microcrack growth in an  $\alpha$  phase involving a large number of cycles and not by the instantaneous spread of an original facet. Microcracks are produced as a Mode II crack where shear slips must be accompanied, and their growth and/or coalescence as shown in Fig. 5(f). Result of 3D analysis in Fig. 6(b) supports the model of microcracking (region A) and its growth (region B). The feature of internal crack initiation sites is not brittle at all but rather ductile, since there

are seen traces of slip. Localized slip and/or slip off, therefore, may play an important role on microcracking and its growth.

#### 4. CONCLUSIONS

Microstructure and internal fatigue crack initiation sites of a Ti-Fe-O alloy were characterized. The results are as follows;

- (1) The microstructure consisted of recovered  $\alpha$  grain and recrystallized  $\alpha$  grain.  $\beta$  phase was distributed along  $\alpha$  grain boundaries with iron enriched.
- (2) The internal crack initiation site was transgranularly formed, and was fitted to a recrystallized  $\alpha$  grain judging from its size, morphology and chemistry.
- (3) Characterized results of crack initiation sites and sub-cracks suggested that a microcracking and its growth in the recrystallized  $\alpha$  grain generated the initiation site.

#### 5. REFERENCES

1. P. Neuman: *Acta Metall.*, vol. 17, 1969, pp. 1219-1225.
2. O. Umezawa and K. Nagai: *Iron Steel Inst. Jpn. Inter.*, vol. 37, 1997, pp. 1170-1179.
3. H. Yokoyama, O. Umezawa, K. Nagai and T. Suzuki: *Iron Steel Inst. Jpn. Int.*, vol. 37, 1997, pp. 1237-1244.
4. J. Ruppen, P. Bhowal, D. Eylon, and J. McEvily: *Fatigue Mechanisms, Spec. Tech. Pub. 675*, 1978, ASTM, Philadelphia, pp. 47-68.
5. O. Umezawa, K. Nagai, and K. Ishikawa: *Fatigue 90, H. Kitagawa and T. Tanaka (eds.)*, 1990, Mater. Component Eng. Pub., Birmingham, UK, vol. 1, pp. 267-272.
6. O. Umezawa, H. Yokoyama, K. Nagai, T. Suzuki, and K. Kokubo: *Fatigue 99, X.R. Wu and Z.G. Wang (eds.)*, 1999, EMAS, in the press.